Neuregulin-1 compensates for endothelial nitric oxide synthase deficiency

Neuregulin-1 Compensates for Endothelial Nitric Oxide Synthase Deficiency

Hadis Shakeri[1], Jente R.A. Boen[1,2], Sofie De Moudt[1], Jhana O. Hendrickx[1], Arthur J.A. Leloup[1], Griet Jacobs[1], Guido R.Y. De Meyer[1], Gilles W. De Keulenaer[1,3,*], Pieter-Jan D.F. Guns[1,*], Vincent F.M. Segers[1,4,*]

[1]Laboratory of Physiopharmacology, University of Antwerp, Universiteitsplein 1, 2610 Antwerp, Belgium.
[2]Research group Cardiovascular Diseases, GENCOR Department, University of Antwerp, Antwerp, Belgium
[3]Hartcentrum ZNA, Antwerp, Belgium.
[4]Department of Cardiology, University Hospital Antwerp, Belgium.
[*]Contributed equally

Corresponding Author: Vincent F.M. Segers M.D. Ph.D.
Universiteitsplein 1, Building D.T.230
2610 Wilrijk, Belgium
Phone: +3232659138, Fax: +3232652412
Email: vincent.segers@uantwerpen.be

Running title: NRG1 Compensates for eNOS deficiency

Abbreviations

Ang II	Angiotensin II
ECs	Endothelial cells
eNOS	Endothelial NO synthase
$eNOS^{-/-}$	eNOS null, eNOS deficient, eNOS knock out
ERBB	Erythroblastic leukaemia viral oncogene homolog
ERK	Extracellular signal-regulated kinase (ERK)
NO	Nitric oxide
NRG1	Neuregulin-1
rhNRG1	Recombinant human neuregulin-1
WT	Wild type

New & Noteworthy

- ECs compensate for eNOS deficiency by increasing the secretion of NRG1.
- NRG1 administration prevents cardiac and renal hypertrophy and fibrosis caused by Ang II infusion and eNOS deficiency.
- NRG1 expression is regulated by miR-134.

Abstract

Endothelial cells (ECs) secrete different paracrine signals that modulate the function of adjacent cells; two examples of these paracrine signals are nitric oxide (NO) and neuregulin-1 (NRG1), a cardioprotective growth factor. Currently, it is undetermined whether one paracrine factor can compensate for the loss of another. Herein, we hypothesized that NRG1 can compensate for endothelial NO synthase (eNOS) deficiency.

Methods. We characterized eNOS null and wild type (WT) mice by cardiac ultrasound and histology and we determined circulating NRG1 levels. In a separate experiment, 8 groups of mice were divided into 4 groups of eNOS null mice and wild type (WT) mice; half of the mice received angiotensin II (Ang II) to induce a more severe phenotype. Mice were randomized to daily injections with NRG1 or vehicle for 28 days.

Results. eNOS deficiency increased NRG1 plasma levels, indicating that ECs increase their NRG1 expression when NO production is deleted. eNOS deficiency also increased blood pressure, lowered heart rate, induced cardiac fibrosis, and affected diastolic function. In eNOS null mice, Ang II administration increased cardiac fibrosis, but also induced cardiac hypertrophy and renal fibrosis. NRG1 administration prevented the cardiac and renal hypertrophy and fibrosis caused by Ang II infusion and eNOS deficiency. Moreover, *Nrg1* expression in the myocardium is shown to be regulated by miR-134.

Conclusion. This study indicates that administration of endothelium-derived NRG1 can compensate for eNOS deficiency in the heart and kidneys.

Key words: Neuregulin-1, Fibrosis, Hypertrophy, Angiotensin II, NO signaling

1 Introduction

Morphologically, the endothelium is the largest continuous organ system and lines the vessels in all tissues. (1, 2) Functionally, the endothelium regulates tissues by secreting multiple paracrine factors, including nitric oxide (NO), which is produced by endothelial nitric oxide synthase (eNOS). (3, 4) Decreased eNOS activity is the cornerstone of endothelial dysfunction and is associated with different cardiovascular disorders, including high blood pressure and cardiac hypertrophy. (4–10) Moreover, eNOS is crucial for normal kidney function, as it has been shown that loss of NO causes glomerulosclerosis, tubular apoptosis, and interstitial fibrosis. (11–14)

Besides NO, endothelial cells (ECs) produce many other paracrine factors—including small molecules, peptides, and proteins—that modulate the function of adjacent cells in different organs, including the heart and kidneys. (4) An important example is neuregulin-1 (NRG1), an endothelium-derived growth factor, which activates ERBB3 (ERBB Receptor Tyrosine Kinase 3) and ERBB4 receptors localized on adjacent tissue cells. (15–18) NRG1 plays crucial roles in cardiovascular and renal development, and induces growth and differentiation of different cell types. (5, 19, 28, 20–27) The cardioprotective effects of NRG1 are well established, (9, 18, 37, 38, 29–36) and a phase 3 clinical trial is ongoing in patients with systolic heart failure (NCT03388593). Recent studies in kidney physiology indicate that disrupted ERBB signaling leads to fibrotic injury, polycystic kidney diseases, and kidney cancer, (39–41) and that NRG1 has protective effects on the kidneys in a mouse model of type-1 diabetes mellitus. (39)

Although the protective effects of many endothelium-derived factors have been studied in detail separately, an open question remains whether ECs modulate secretion of one paracrine factor in case another paracrine factor is abrogated; *i.e.*, if one paracrine factor is downregulated, will ECs compensate by increased production of another paracrine factor? A second question is whether exogenous administration of this other factor can compensate for the initial defect.

To test the specific hypotheses that ECs respond to endothelial NO synthase (eNOS) deficiency by increasing their production of NRG1, we first characterized cardiac function, morphology, and NRG1 levels in eNOS null mice compared to wild type (WT) mice. To test the hypothesis that exogenous administration NRG1 can compensate for eNOS deficiency, we

performed another experiment (in WT and eNOS null mice) in which we added Ang II infusion to half of the groups to increase the severity of the model. Although the cardioprotective effects of the endothelium-derived paracrine factors NO and NRG1 have been well studied separately, the interaction between both has never been studied before.

2 Materials & methods

2.1 Animal models. All animal experiments were approved by the institutional ethics committee of the University of Antwerp and conform to the Guide for the Care and Use of Laboratory Animals published by the US National Institute of Health (Updated version 2011). 15–16-week-old eNOS knock-out mice (The Jackson Laboratory, male and female, eNOS null mice; N=42) (42–44) and their wild type littermate control mice (WT, male and female; N=42) were used in 2 separate experiments to determine cardiac function by ultrasound, hypertrophy and fibrosis of the heart and kidneys, and NRG1 levels. In the second experiment, osmotic minipumps (ALZET, model 2004) filled with Ang II (400 ng/kg.min, Sigma Aldrich) (45) were implanted for 28 days—to induce a more severe phenotype—in half of the eNOS null mice and WT mice under general anesthesia (3% isoflurane), while the other half of the mice underwent sham surgery. Mice were randomized to receive either daily recombinant human NRG1 (rhNRG1) injections (20 µg/kg.day, intraperitoneal, Peprotech) or vehicle (PBS) for 4 weeks, starting on the day of surgery. (18) The dose of NRG1 was based on previous studies. (18, 46, 47)

Cardiac ultrasound (Vevo 2100, VisualSonics) and blood pressure measurements (Coda, Kent Scientific) were performed in week 4 of the experiment. Cardiac ultrasound was used to asses systolic and diastolic function, as well as cardiac dimensions including LV mass, which was calculated according to the formula: LV mass = (0.8*(1.04*((LVEDD+IVSd+LVPWd)^3 - LVEDD^3)))+0.6. At the end of 4th week, mice were euthanized using pentobarbital (100 mg/kg, intraperitoneal, CEVA Santé Animale). Blood was collected from the periorbital venous sinus. The apex of the heart was fixed in tissue embedding medium (NEG 50, ThermoFischer Scientific), the mid part was fixed in 4% buffered formalin and embedded in paraffin, and the basal segment of the heart was snap frozen for Western blot analyses. The left kidney was cut longitudinally in 2 pieces and embedded in NEG 50 and paraffin. The right kidney was snap frozen for Western blot analyses.

2.2 Histology. Paraffin embedded heart and kidney sections were stained with Masson's trichrome to measure fibrosis. Fibrosis was measured on the total area of heart and kidney sections, as well as in glomeruli and perivascular area; 10 glomeruli and 6 micro vessels were randomly analyzed. Cardiomyocyte borders were visualized using both laminin staining (Novus Biologicals) and fluorescent wheat germ agglutinin lectin (WGA, Invitrogen, Alexa Fluor 594) and cardiomyocyte cross sectional area—at the level of the nucleus—was calculated by averaging 25 random cardiomyocytes per image per animal (5 images per

animal). Isolectin staining (Isolectin IB, Alexa Fluor, Invitrogen) and DAPI staining was performed on cardiac tissue for visualization of capillaries to determine capillary density, which was calculated as the average number of capillaries/mm². A total of 3 images per animal was used. Apoptosis was visualized by staining with antibodies specific for cleaved caspase 3 (Cell Signaling) and with TUNEL assay kit (ApopTag Plus Peroxidase In situ Apoptosis Detection kit, Merck). Images were acquired with an Olympus microscope and Nikon eclipse Ti fluorescence microscope and analyzed with ImageJ software.

2.3 Western blotting. Heart and kidney sections were incubated in Radioimmunoprecipitation assay lysis buffer (RIPA, Sigma) supplemented with protease and phosphatase inhibitors (complete Mini and PhosSTOP, Roche) on ice for 5 min and mixed using a Precellys 24 tissue homogenizer (Bertin Instruments). After centrifugation, to pellet non-dissolved material, protein concentration of the supernatant of each sample was determined using the bicinchoninic acid method (BCA, ThermoFischer). Equal amounts of protein were separated on Bolt 4–12% bis-tris gels (Invitrogen) and blotted onto polyvinylidene fluoride membranes. Membranes were blocked in Odyssey Blocking Buffer (Li-Cor Biosciences) and probed with primary antibody (overnight, 4°C). Following primary antibodies were used: rabbit anti p44/42 MAPK (Erk1/2, Cell Signaling 4695, 42,44 kDa, 1:1000) and rabbit anti phospho-p44/42 MAPK (Erk1/2, Thr202/Tyr204, Cell Signaling 4377, 42,44 kDa, 1:1000), and GAPDH (Cell Signaling 5174, 37 kDa, 1:2000). Subsequently, infrared fluorescence (IR)-conjugated secondary antibodies (anti-rabbit: IgG926-32211 and anti-mouse IgG926-68070; Li-COR Biosciences, 1:20000) were used for IR fluorescence detection using an Odyssey SA IR imaging system (Li-COR Biosciences). Each Western blot panel pictured in this article was derived from one single continuous blot.

2.4 Urinary albumin analysis. Urine was collected during a 24-hour period in metabolic cages and stored at -80°C. Urinary albumin was measured using a mouse albumin ELISA kit (Bethyl Laboratories) according to manufacturer's protocol and with a 10000 fold dilution. Urinary creatinine concentration was measured using a clinical grade autoanalyzer (Siemens Vista 1500, Laboratory of Clinical Biology at the Antwerp university hospital).

2.5 ELISA of NRG1 in plasma. Immediately after sacrifice, heparinized blood was centrifuged at 14,000 rpm at 4°C for 15 min and plasma was separated from debris. Plasma NRG1 was measured using a mouse NRG1 ELISA kit (Bethyl Laboratories) according to manufacturer's protocol. Plasma samples were used without any dilution.

2.6 miRNA analysis *in vivo*. Two miRNA target gene prediction tools were used to find miRNAs targeting *NRG1* in human and mouse: miRSystem and miRWalk. miRSystem is a database which integrates seven miRNA target gene prediction programs: DIANA, miRanda, miRBridge, PicTar, PITA, rna22, and TargetScan. (48–50) The miRWalk database contains information produced with TarPmiR, a miRNA-mRNA binding site prediction tool that applies a random-forest-based approach. Next, expression of the NRG1-targeting miRNAs was checked in the TissueAtlas database, with focus on veins, arteries, hearts, and kidneys of human biopsy samples. The 4 miRNAs—miR-16, miR-24, miR-134, and miR223—with the highest mean expression in these 4 organs were evaluated in WT and eNOS-null mice with qPCR. Total RNA was isolated (Mirvana kit, Invitrogen) from OCT embedded heart sections of Ang II–injected animals (WT; N=8 and $eNOS^{-/-}$; N=7) using Precellys Homogenizer device. Cardiac expression of the miRNA panel (miR-16-5p, miR-24-3p, miR-134-5p, miR-223-3p) was quantified with qPCR, using TaqMan PreAmp Master Mix (Applied Biosystems), TaqMan Universal Master Mix II no UNG (Applied Biosystems), and TaqMan primers (Life Technologies). All samples were normalized to RNU6B and relative log fold change expression was calculated using $\log(2^{-(\Delta\Delta cT)})$ method in R.

2.7 *In vitro* experiments with miRNA-134 inhibitor. Primary mouse cardiac ECs were obtained via magnetic bead isolation from C57BL/6 mice (Neonatal Cardiac Endothelial Cell Isolation Kit, Miltenyi Biotec). Cells were cultured in DMEMF12 supplemented medium at 37°C, 5% CO_2. Cells were seeded at a density of 20,000 cells/well in a 96 well plate. Mmu-mir-134-5p power inhibitor (700nM, Qiagen) was added to the cells according to the manufacturer's protocol, followed by the addition of 1μM of Ang II (Sigma Aldrich, A9525). Cells were treated for 48 hours, after which total RNA was isolated (MirVana Kit, Invitrogen). mRNA expression levels of *Nrg1* were determined using RT-qPCR. All samples were normalized to β-actin (Mm00607939-s1, Life Technologies), while relative fold change expression was calculated using the $\log(2^{-(\Delta\Delta CT)})$ method.

2.8 Reverse transcription quantitative polymerase chain reaction of *Nppa* and *Nppb*. To determine expression of *Nppa* (coding for atrial natriuretic peptide, ANP) and *Nppb* (coding for brain natriuretic peptide, BNP), cardiac tissue was homogenized using a Precellys 24 Homogenizer (Bertin Instruments). RNA was isolated with the Nucleospin RNA isolation kit (Filter Service) according to the manufacturer's protocol. Reverse transcription was performed using TaqMan™ Reverse Transcription Reagents (Invitrogen), followed by quantification on PCR using TaqMan™ Universal PCR Master Mix (Applied Biosystems)

and TaqMan primers (*Nppa*: mm01255747_g1; *Nppb*:mm01255770_g1, Life Technologies) on a Quant Studio 3 qPCR device. *Actb* (coding for beta-actin) was used as a house keeping gene, while relative expression was calculated according to the $\log 2^{(-\Delta\Delta CT)}$ method.

2.9 Statistical analysis. All data were analyzed using Graph-pad Prism software version 8.0, and presented as Mean±SEM. Student's T test was used for comparison between two genotypes (WT or $eNOS^{-/-}$) and Two-way ANOVA was used for each genotype separately (WT or $eNOS^{-/-}$) and a Bonferroni correction for multiple comparison was used in post-hoc tests. In case of non-normal distribution; logarithmic transformation of the data was performed. Statistical significance was defined as $P < 0.05$.

3 Results

3.1 eNOS deletion increases NRG1 plasma levels. We first determined whether NRG1 increases upon eNOS deletion, by measuring NRG1 protein levels in the circulation. NRG1 protein levels were 5-fold higher in blood plasma of eNOS null mice (Fig. 1A). eNOS deletion did not induce cardiomyocyte hypertrophy (Fig. 1B), but led to significant changes in interstitial fibrosis in the heart (Fig. 1C), heart rate (Fig. 1D), and in a number of ultrasound measurements of diastolic function: isovolumic relaxation time (IVRT), early (E), and late (A) filling rate (Fig. 1I–J). eNOS deletion did not change ventricular ejection fraction or cardiac mass (Fig. 1E–G).

3.2 eNOS deletion, but not chronic infusion of a low dose of Ang II, increases blood pressure. Next, we aimed to study whether NRG1 could compensate for the loss of NO. However, because the phenotype of eNOS null mice was mild and limited to myocardial fibrosis without hypertrophy, we decided to include groups receiving a chronic infusion of Ang II which induces a more severe phenotype with cardiac hypertrophy. We used a low dose of Ang II—called a *subpressor* dose because of limited effects on blood pressure—to limit the high mortality rate observed with higher doses of Ang II in eNOS null mice. (45) Although eNOS null mice showed a higher blood pressure compared to their WT mice, *subpressor* doses of Ang II or NRG1 treatment did not affect blood pressure (Fig. 2A–C); this indicates that the effects observed in this study are largely blood pressure independent. The mortality rate was higher in eNOS null animals compared to WT animals, when treated with Ang II (Fig. 2D), but not statistically significant (33% in $eNOS^{-/-}$ +Ang II vs. 11% in WT +Ang II group). NRG1 did not significantly affect the mortality in this study. No mortality was observed in animals without Ang II treatment, independent of their genotype.

3.3 NRG1 administration compensates for eNOS deficiency in Ang II–induced cardiac hypertrophy. *Subpressor* doses of Ang II induced a more severe cardiac phenotype, and this phenotype was still dependent on eNOS levels, *i.e.* it was milder in WT mice, allowing us to study whether NRG1 could compensate for the loss of NO. Specifically, in WT mice, the effects of *subpressor* doses of Ang II on cardiac hypertrophy were small and statistically non-significant (Fig. 3B, C). However, when eNOS was deleted, *subpressor* doses of Ang II induced a hypertrophic response, as shown by a significantly increased intraventricular septum thickness (Fig. 3B) and increased post-mortem heart-to-body weight (Fig. 3C). Importantly, daily administration of NRG1 completely compensated for the hypertrophic

responses induced by eNOS deficiency upon *subpressor* doses of Ang II (Fig. 3B, C). Left ventricular end-diastolic volume was similar in all groups (Fig. 3D), and heart rate was slower in eNOS null mice than in WT mice, but not affected by administration of either Ang II or NRG1 (Fig. 3E). *Nppb*, coding for BNP, a marker of cardiomyocyte strain, was not differentially expressed in cardiac tissues. In contrast, *Nppa*, coding for ANP, showed an upregulation in eNOS null mice treated with NRG1 (Fig3. F, G). Administration of NRG1 prevented the increase in cardiomyocyte cross sectional area (Fig. 3H, I), induced by the combination of Ang II infusion and eNOS deficiency as defined by laminin staining (Fig. 3H). The same trend was observed with wheat germ agglutinin staining, with a significant group effect of NRG1 in eNOS null mice (P=0.02; two-way ANOVA; Suppl. Fig. 1).

3.4 NRG1 administration compensates for eNOS deficiency in Ang II–induced cardiac fibrosis. Deficiency of eNOS combined with Ang II administration also led to significantly higher interstitial fibrosis (Fig. 4A, C)—and NRG1 treatment suppressed this fibrotic response (+Ang II +NRG1, Fig. 4B). eNOS deficiency combined with Ang II administration also led to significantly increased perivascular fibrosis, which was again attenuated by NRG1 treatment (Fig. 4C, D). No significant differences in myocardial capillary density were observed between the different groups (Fig. 4E, F).

3.5 NRG1 administration compensates for eNOS deficiency in Ang II–induced renal albuminuria, hypertrophy, and fibrosis. To determine whether the compensatory effects of NRG1 to eNOS deficiency are cardiac-specific or system-wide, we also examined renal function and morphology, because ECs have an important functional role in the kidney. First, we measured albuminuria, because it often is the first sign of kidney dysfunction. eNOS deficiency, even in the absence of Ang II, significantly increased albuminuria—quantified by the relative urinary albumin concentration normalized to urinary creatinine concentration, and this effect was accentuated when eNOS deficiency was combined with Ang II administration (Fig. 5A). Here, NRG1 treatment only partly normalized albuminuria (Fig. 5A).

Second, NRG1 significantly reduced kidney weight in eNOS null mice, regardless of Ang II administration (Fig. 5B). The glomerulus is a network of capillaries and histologically defined as a tuft. An increase in glomerular tuft area corresponds to an increased glomerular volume and is a key pathological finding in glomerulosclerosis. (51) Both eNOS deficiency and Ang II administration increased glomerular tuft area significantly, with the highest areas measured when combined (Fig. 5C, D). Administration of NRG1 compensated for eNOS deficiency,

277 both in the presence and absence of Ang II.

278 Third, eNOS deficiency and Ang II administration significantly increased fibrosis on total
279 sections of kidneys (Fig. 5E, F). Specifically, in glomeruli, the fibrotic response to eNOS
280 deficiency and Ang II was most pronounced (Fig. 5G), indicating most damage at this stage
281 primarily occurs in the glomeruli. Again, administration of NRG1 compensated for this
282 fibrosis induced by eNOS deficiency, Ang II administration, and the combination of both
283 (Fig. 5H). Together with the data in the heart, these data indicate that the compensatory
284 effects of NRG1 for eNOS deficiency on fibrosis are preserved in different organs.

285 **3.6 NRG1 administration compensates for eNOS deficiency–induced Erk**
286 **phosphorylation and vascular apoptosis.** The previous sections showed that administration
287 of NRG1 can compensate for the lack of NO in terms of tissue function, hypertrophy, and
288 fibrosis. Here, we questioned whether these compensatory effects could be traced to
289 subcellular signaling pathways and apoptotic pathways. First, the extracellular signal-
290 regulated kinase (Erk) pathway is a paramount pathway for tissue homeostasis in the heart.
291 (52) Western blot analysis of the myocardium showed that Ang II administration, eNOS
292 deficiency, or both together increased phosphorylation of Erk1/2 (Fig. 6A). Administration of
293 NRG1 compensated significantly for eNOS deficiency-induced phosphorylation of Erk1/2
294 (Fig. 6B). Second, eNOS deficiency induced a significantly higher level of apoptosis—
295 determined by cleaved caspase 3 staining (Fig. 6C)—in intramural cardiac arteries with or
296 without Ang II infusion. NRG1 treatment significantly reduced vascular apoptosis induced by
297 eNOS deficiency (Fig. 6D). No apoptosis was observed in cardiomyocytes. TUNEL staining
298 on cardiac tissue also showed no significant differences in cardiomyocyte apoptosis between
299 the different groups (P=0.87 in WT and P=0.95 in eNOS null mice). In summary, the
300 compensatory effects of NRG1 administration on eNOS deficiency can be traced to
301 subcellular signaling and apoptotic pathways.

302 **3.7 *Nrg1* expression is, in part, regulated by miR-134.** It is currently undetermined which
303 miRNAs regulate *Nrg1* expression in ECs. Therefore, two miRNA target gene prediction
304 tools were used to discover miRNAs targeting *NRG1* in human and mouse: miRSystem and
305 miRWalk. The miRSystem database resulted in 20 miRNAs predicted to bind both human and
306 mouse *NRG1* mRNA and the miRWalk database resulted in 53 miRNAs predicted to bind
307 both human and mouse *NRG1* mRNA; three of these miRNAs were identical. Expression of
308 these 70 miRNAs in veins, arteries, hearts, and kidneys—organs with a large fraction of

ECs—of human biopsy samples was checked in the TissueAtlas database. 27 miRNAs showed significant expression in these organs and the four miRNAs—miR-16, miR-24, miR-134, and miR223—with the highest mean expression in these organs were evaluated in cardiac tissues of WT and eNOS null mice with qPCR. All four miRNAs were downregulated in eNOS null hearts—which is consistent with the theory that these miRNAs inhibit *Nrg1* expression—but only the downregulation of miR-134 was significant (Fig. 7A). Next, we tested whether a miR-134 inhibitor increases *Nrg1* expression in ECs *in vitro*, which was not the case in basal conditions (Fig. 7B). However, the miR-134 inhibitor did result in a mild increase in *Nrg1* expression in ECs, when stimulated with Ang II (Fig. 7C).

Data supplements: https://doi.org/10.5281/zenodo.4749643

4 Discussion

The endothelial system occupies an unique position at the interface between the individual organs and the circulating blood and regulates overall homeostasis by affecting all organs in the body. (4, 53, 54) The most studied role of the endothelial system has been its control of vasomotoricity and organ perfusion by interacting of ECs with subjacent smooth muscle cells. More importantly, however, ECs are also present in capillaries, which constitute the largest endothelial surface in every organ. In capillaries, ECs directly communicate with adjacent tissue cells, such as neurons, alveolar cells, cardiomyocytes, tubular and glomerular cells in the kidney, hepatocytes, and fat cells. (4, 53, 54) The endothelial system is an adaptive system that can undergo dramatic changes in gene expression during development and disease. (55)

Although the protective effects of many endothelium-derived factors have been studied in detail, an open question remains whether ECs modulate secretion of one paracrine factor in case another paracrine factor is abrogated and whether supplementary administration of this other factor can compensate for the initial defect. In this study, we tested the specific hypotheses that ECs will respond to eNOS deficiency by increasing their production of NRG1 and that administration of NRG1 can compensate for eNOS deficiency. Summarized, this study provides evidence that ECs increase the release of NRG1 upon eNOS deficiency, albeit insufficient to prevent a pathophysiological phenotype, but that administration of *extra* NRG1 can compensate for the negative effects of diminished NO/eNOS signaling.

For this study, we selected two important endothelial-derived paracrine factors with proven physiological relevance and with different underlying signaling pathways. First, we selected NO, because it is well known that NO has crucial roles in the regulation of various physiological processes. (56) NO is synthesized from L-arginine mediated by the NOS family, which includes neuronal NOS (nNOS) in neural tissue, inducible NOS (iNOS) in macrophages, and endothelial NOS (eNOS) in the endothelium. (57) Reduced NO bioavailability is the hallmark of endothelial dysfunction, which contributes to different cardiovascular diseases including high blood pressure, cardiac hypertrophy, cardiac remodeling, and atherosclerosis. (4, 5, 58–62) A disrupted NO/eNOS signaling is also associated with different kidney disorders, such as glomerulosclerosis, interstitial fibrosis, diabetic nephropathy, and cardiorenal syndrome. (11) It has been shown previously that eNOS null mice display normal cardiac function and ejection fraction when young, but develop cardiac dysfunction at older age. (44) Our data are also consistent with earlier reports

showing decreased heart rate and increased blood pressure in eNOS null mice. (43) Second, we selected NRG1, an epidermal growth factor that is produced by ECs and that exerts its effect via ERBB tyrosine kinase receptors. (17) NRG1 plays a crucial role in cardiac development and pathophysiology, and has anti-apoptotic and anti-fibrotic effects. (10, 16, 18) Moreover, NRG1 has been shown to attenuate heart failure in several animal models and is currently under evaluation as a potential treatment for heart failure in a phase 3 clinical trial. (36, 37)

We have previously reported that NRG1 attenuates Ang II-induced myocardial hypertrophy and fibrosis in model of Ang II-induced hypertension in the mouse. (18) These observations are partly recapitulated in this study. The difference of the present study is that we used a low subpressor dose of Ang II, which did not induce the full picture of abnormalities in the heart and kidneys observed with higher hypertension-inducing doses of Ang II. Only in mice where eNOS was absent, subpressor Ang II doses induced myocardial fibrosis, myocardial hypertrophy, kidney fibrosis, and albuminuria, which confirms the protective role of NO in heart and kidney. An interesting observation in this study is that NRG1 stimulated *Nppa* expression in cardiac tissue of eNOS null mice; because ANP has protective properties in the heart and the kidneys, (63) one could speculate that part of the beneficial effects of NRG1 might be mediated by increased ANP levels. The main finding of the present study is that NRG1 can compensate for NO when hypertrophic and fibrotic tissue responses are initiated due to lack of NO.

Another conclusion of this study is that, although NRG1 levels were robustly induced in eNOS null mice in the circulation, this upregulation is insufficient to prevent a pathophysiological phenotype of hypertrophy and fibrosis. However, the fact that the upregulation does not prevent a phenotype does not mean that the upregulation of NRG1 has no physiological relevance. Compensatory pathways in biology almost never reverse detrimental effects of deletion of an important signaling pathway. It is conceivable that, without compensatory upregulation of NRG1, the phenotype of eNOS null mice would be even more severe. An example supporting this claim is the finding that *Nrg1* deletion in endothelial cells worsens the cardiac phenotype after ischemia/reperfusion injury. (64)

A next conclusion of this study is that the cardio- and nephro-protective effects of NRG1 are independent of the eNOS pathway. To some extent, this finding is surprising because there are indirect indications in the literature that some of the cardioprotective effects of NRG1 are

mediated by eNOS activation. (5, 35) Especially since NRG1 has been shown to induce phosphorylation of endothelial NO synthase and nitrite production in cardiomyocytes. The precise cell and tissue-protecting effects are still largely unknown, although anti-apoptotic and anti-inflammatory effects have been postulated.

Interestingly, in this study we show that the compensatory effects of NRG1 administration on eNOS deficiency can be traced to subcellular signaling and apoptotic pathways. We selected the Erk pathway because it is involved in hypertrophy (65) and selected cleaved caspase-3 because it is involved in cell-death pathways. However, it is likely that the compensatory effects of NRG1 go beyond these two pathways and affect many other subcellular signaling pathways involved in hypertrophy and fibrosis. With regard to myocardial capillary density, our results are in line with previous studies showing that eNOS null mice at adult age are indistinguishable from their WT littermates. In contrast, neonatal eNOS null mice have a lower capillary density. (42) It has been shown in a rat model of diabetic cardiomyopathy that NRG1 can induce expression of vascular endothelial growth factor (VEGF), (66) which can induce cardiac and renal protection (67) in a dose-dependent manner. (68) However, in contrast to these earlier studies, we did not observe increased capillary density upon exogenous NRG1 administration. The reason for this discrepancy is unclear, yet the lack of angiogenic abnormalities in the animal model used in the present study might prevent the detection of NRG1-associated proangiogenic activity. In relation to EC signaling, we also show that miR-134 is a regulator of *Nrg1* expression in ECs, nevertheless it is likely that many other miRNAs are involved as well. Despite the identification of the miR-134/*Nrg1* regulatory axis at the RNA level, no results were obtained at the protein level, which is a limitation of the present study.

Consistent with the data from the present paper, data from human studies have been published showing that circulating NRG1 levels are upregulated in patients with coronary artery disease and heart failure—two diseases characterized by endothelial dysfunction. (69–71) These data indicate that our study could also be relevant in human disease. Wider ranging implications could result from the fact that pharmacological stimulation of one endothelial pathway can compensate for a defect in another endothelial pathway. The therapeutic implications could be that—even when one pathway is the main driver of kidney failure or heart failure—it is still worthwhile to try to compensate by targeting other pathways.

Finally, it has recently been claimed by Zurek et al. that NRG1 induces cardiac hypertrophy

in post–myocardial infarction rats. (72) This claim was based on a mere increase in ventricular mass—calculated by MRI—at a single dose (2.5μg/kg/h for 7 days); both lower and higher doses did not induce hypertrophy. The data of Zurek et al. contradict the anti-hypertrophic response induced by NRG1 that was observed in the present study, as well as in several previous studies. (18, 73) Importantly, in this study we demonstrated the anti-hypertrophic effect of NRG1 using three well-established parameters of hypertrophy: interventricular septum thickness using cardiac ultrasound, post-mortem heart weight, and cardiomyocyte cross sectional area using histology.

5 Conclusions

This study indicates that endothelial-derived NRG1 can function as a compensatory pathway for eNOS deficiency, but also that the natural upregulation of NRG1 is inadequate. The compensatory effects of NRG1 for eNOS deficiency appear to be present in the endothelial system throughout the organism. Translational implications are that administration of endothelial-derived factors could be therapeutically effective, even if the underlying defect involves a different paracrine factor.

6 Author Contributions

VFM. Segers, G.W. De Keulenaer, P-J.D.F. Guns, and H. Shakeri designed research; H. Shakeri, S. De Moudt, J.R.A. Boen, A.J. Leloup, J.O. Hendrickx, and G. Jacobs performed research; H. Shakeri, J.R.A. Boen, S. De Moudt, G. Jacobs, and J. Hendrickx analyzed data; V.F.M. Segers, P-J.D.F. Guns, G.W. De Keulenaer, G.R.Y. De Meyer, and H. Shakeri wrote the paper; all authors read and approved the final version.

7 Acknowledgments

We would like to thank Rita Van Den Bossche and Tine Bruyns for technical support. This work was supported by a DOCPRO4 grant (PID29621), an IOF/SBO research grant (PID34923), and a GOA grant (PID36444) of the University of Antwerp; by a Senior Clinical Investigator fellowship (to VFS) and research grants of the Fund for Scientific Research Flanders (Application numbers 1842219N, G021019N, and G021420N); by a research grant of ERA.Net RUS Plus (2018, Project Consortium 278).

Figure legends

Figure 1. eNOS deletion increases NRG1 levels and myocardial fibrosis. A) NRG1 levels in plasma measured using ELISA for mouse NRG1 in eNOS deficient mice ($eNOS^{-/-}$) and compared to the control group (N=5). B) Cardiomyocyte cross sectional area, C) cardiac fibrotic area, and D) heart rate. Cardiac function was assessed by ultrasound: E) end-diastolic interventricular septal thickness (IVS;d), F) left ventricular mass (LV mass), G) ejection fraction (EF), H) isovolumic relaxation time (IVRT), I) left ventricular end-diastolic volume (LV-EDV), J) early filling velocity (E), K) late filling velocity (A), and L) early diastolic mitral annular tissue velocity (é). N=10 in B–L; Student's t-test; *P<0.05.

Figure 2. Chronic infusion of a low dose of Ang II has no effect on blood pressure and mortality. A) Systolic blood pressure, B) diastolic blood pressure, and C) mean arterial pressure (MAP) measured by tail-cuff method. D) The effect of Ang II treatment on mortality in WT and $eNOS^{-/-}$ animals. Graphs show both WT and eNOS-/- animals with and without Ang II infusion (AngII and Ctrl). Each group treated with and without NRG1 (NRG1 and vehicle). N=8 per group; mean±SEM; two-way ANOVA.

Figure 3. Administration of NRG1 compensates completely for Ang II- and eNOS deficiency-induced cardiac hypertrophy. A) Ejection fraction (EF) and B) diastolic intraventricular septum thickness (IVS;d) measured by cardiac ultrasound. C) Post-mortem heart weight normalized to body weight. D) Left ventricular end-diastolic volume measured by ultrasound. E) Heart rate measured by CODA. mRNA expression levels of F) *Nppa* and G) *Nppb*. H) Representative microscopic images of laminin staining of the heart used for quantification of cross sectional area. I) Quantification of cardiomyocyte cross sectional area. N=8 per group; mean±SEM; two-way ANOVA with Bonferroni correction for multiple comparisons; *P<0.05; **P<0.01.

Figure 4. Administration of NRG1 compensates for Ang II- and eNOS deficiency-induced cardiac fibrosis. A & C) Representative microscopic images of Masson's trichrome staining (blue colour) of the heart to measure B) interstitial fibrosis in the total heart; and D) perivascular fibrosis. E) Isolectin staining (green) and DAPI staining (blue) of the heart to determine F) capillary density/mm². N=8 per group; Mean±SEM; two-way ANOVA with Bonferroni correction for multiple comparisons; *P<0.05; ***P<0.001; #P<0.05 compared to WT, ##P<0.01 compared to WT.

Figure 5. Administration of NRG1 compensates for Ang II- and eNOS deficiency-induced renal albuminuria, hypertrophy, and fibrosis. A) Amount of urinary albumin normalized by the urinary creatinine, measured from samples collected in 24 hours. B) Kidney weight/body weigh at the end of the experiment. C) Representative images of periodic-acid Schiff staining used to measure D) the size of the glomerular tuft area. E) Representative images of Masson's trichrome staining on total kidney and G) glomeruli, indicating F) renal interstitial fibrosis and H) glomerular fibrosis (blue color). N=8 per group; Mean±SEM; two-way ANOVA with Bonferroni correction for multiple comparisons; *P<0.05; **P<0.01; ***P<0.001.

Figure 6. Administration of NRG1 compensates for eNOS deficiency-induced Erk phosphorylation and vascular apoptosis. A) Western blots of heart samples using antibodies against Erk1/2 and phosphorylated Erk1/2 (p-Erk1/2); GAPDH is used as a protein loading control. B) Analysis of relative band intensity of p-Erk1/2 normalized by the total Erk1/2 protein. C) Representative microscopic images of cleaved-caspase 3 (Cl-casp3) staining of the heart, to measure D) vascular apoptosis. N=8 per group; Mean±SEM; two-way ANOVA with Bonferroni correction for multiple comparisons; *P<0.05.

Figure 7. miR-134 regulates *Nrg1* expression. A) Expression of four miRNAs in cardiac tissue that were predicted to interact with NRG1 in human and mouse and with a high expression in organs with a large fraction of ECs. N WT=7, N $eNOS^{-/-}$ =8; Mean±SEM; Unpaired T-test; *P<0.05. B) In primary cardiac ECs, the miR-134 inhibitor did not change *Nrg1* expression in basal conditions. C) When Ang II was added to all groups (except to the Untreated group), the miR-134 inhibitor induced a mild increase in *Nrg1* expression. N=9 per group. Mean±SEM; one-way ANOVA with Tukey correction for multiple comparisons; *P<0.05.

8 References

1. Aird, W. C. (2004) Endothelium as an organ system. *Crit. Care Med.* **32**, S271–S279
2. Hendrickx, J., Doggen, K., Weinberg, E. O., Van Tongelen, P., Fransen, P., and De Keulenaer, G. W. (2004) Molecular diversity of cardiac endothelial cells in vitro and in vivo. *Physiol. Genomics* **19**, 198–206
3. Brutsaert, D. L. (2003) Cardiac Endothelial-Myocardial Signaling: Its Role in Cardiac Growth, Contractile Performance, and Rhythmicity. *Physiol. Rev.* **83**, 59–115
4. Segers, V. F. M., Brutsaert, D. L., and De Keulenaer, G. W. (2018) Cardiac Remodeling: Endothelial Cells Have More to Say Than Just NO. *Front. Physiol.* **9**, 382
5. Lemmens, K., Fransen, P., Sys, S. U., Brutsaert, D. L., and De Keulenaer, G. W. (2004) Neuregulin-1 induces a negative inotropic effect in cardiac muscle: role of nitric oxide synthase. *Circulation* **109**, 324–326
6. Qian, J. and Fulton, D. (2013) Post-translational regulation of endothelial nitric oxide synthase in vascular endothelium. *Front. Physiol.* **4**, 347
7. Shesely, E. G., Maeda, N., Kim, H. S., Desai, K. M., Krege, J. H., Laubach, V. E., Sherman, P. A., Sessa, W. C., and Smithies, O. (1996) Elevated blood pressures in mice lacking endothelial nitric oxide synthase. *Proc. Natl. Acad. Sci. U. S. A.* **93**, 13176–13181
8. Murad, F. (2004) Discovery of Some of the Biological Effects of Nitric Oxide and its Role in Cell Signaling. *Biosci. Rep.* **24**, 452–474
9. Doggen, K., Ray, L., Mathieu, M., Mc Entee, K., Lemmens, K., and De Keulenaer, G. W. (2009) Ventricular ErbB2/ErbB4 activation and downstream signaling in pacing-induced heart failure. *J. Mol. Cell. Cardiol.* **46**, 33–38
10. Lemmens, K., Doggen, K., and De Keulenaer, G. W. (2011) Activation of the neuregulin/ErbB system during physiological ventricular remodeling in pregnancy. *Am. J. Physiol. Heart Circ. Physiol.* **300**, H931-42
11. Lee, J., Bae, E. H., Ma, S. K., and Kim, S. W. (2016) Altered Nitric Oxide System in Cardiovascular and Renal Diseases. *Chonnam Med. J.* **52**, 81
12. Morisada, N., Nomura, M., Nishii, H., Furuno, Y., Sakanashi, M., Sabanai, K., Toyohira, Y., Ueno, S., Watanabe, S., Tamura, M., Matsumoto, T., Tanimoto, A., Sasaguri, Y., Shimokawa, H., Kusuhara, K., Yanagihara, N., Shirahata, A., and Tsutsui, M. (2010) Complete disruption of all nitric oxide synthase genes causes

markedly accelerated renal lesion formation following unilateral ureteral obstruction in mice in vivo. *J. Pharmacol. Sci.* **114**, 379–389

13. Sun, D., Wang, Y., Liu, C., Zhou, X., Li, X., and Xiao, A. (2012) Effects of nitric oxide on renal interstitial fibrosis in rats with unilateral ureteral obstruction. *Life Sci.* **90**, 900–909

14. Miyajima, A., Chen, J., Poppas, D. P., Vaughan, E. D., and Felsen, D. (2001) Role of nitric oxide in renal tubular apoptosis of unilateral ureteral obstruction. *Kidney Int.* **59**, 1290–1303

15. Lemmens, K., Doggen, K., and Keulenaer, G. W. De. (2008) Neuregulin-1 and its potential role in the control of cardiac function. *Heart Fail. Monit.* **5**, 119–124

16. Lemmens, K., Doggen, K., and De Keulenaer, G. W. (2007) Role of Neuregulin-1/ErbB Signaling in Cardiovascular Physiology and Disease: Implications for Therapy of Heart Failure. *Circulation* **116**, 954–960

17. Parodi, E. M. and Kuhn, B. (2014) Signalling between microvascular endothelium and cardiomyocytes through neuregulin. *Cardiovasc. Res.* **102**, 194–204

18. Vermeulen, Z., Hervent, A.-S., Dugaucquier, L., Vandekerckhove, L., Rombouts, M., Beyens, M., Schrijvers, D. M., De Meyer, G. R. Y., Maudsley, S., De Keulenaer, G. W., and Segers, V. F. M. (2017) Inhibitory actions of the NRG-1/ErbB4 pathway in macrophages during tissue fibrosis in the heart, skin, and lung. *Am. J. Physiol. Circ. Physiol.* **313**, H934–H945

19. Lee, K. F., Simon, H., Chen, H., Bates, B., Hung, M. C., and Hauser, C. (1995) Requirement for neuregulin receptor erbB2 in neural and cardiac development. *Nature* **378**, 394–398

20. Meyer, D. and Birchmeier, C. (1995) Multiple essential functions of neuregulin in development. *Nature* **378**, 386–390

21. Negro, A., Brar, B. K., and Lee, K.-F. (2004) Essential roles of Her2/erbB2 in cardiac development and function. *Recent Prog. Horm. Res.* **59**, 1–12

22. Brown, D., Samsa, L. A., Ito, C., Ma, H., Batres, K., Arnaout, R., Qian, L., and Liu, J. (2018) Neuregulin-1 is essential for nerve plexus formation during cardiac maturation. *J. Cell. Mol. Med.* **22**, 2007–2017

23. Wang, Z., Xu, G., Wu, Y., Guan, Y., Cui, L., Lei, X., Zhang, J., Mou, L., Sun, B., and Dai, Q. (2009) Neuregulin-1 enhances differentiation of cardiomyocytes from embryonic stem cells. *Med. Biol. Eng. Comput.* **47**, 41–48

569 24. Ozcelik, C., Erdmann, B., Pilz, B., Wettschureck, N., Britsch, S., Hübner, N., Chien, K.
570 R., Birchmeier, C., and Garratt, A. N. (2002) Conditional mutation of the ErbB2
571 (HER2) receptor in cardiomyocytes leads to dilated cardiomyopathy. *Proc. Natl. Acad.*
572 *Sci. U. S. A.* **99**, 8880–8885
573 25. García-Rivello, H., Taranda, J., Said, M., Cabeza-Meckert, P., Vila-Petroff, M.,
574 Scaglione, J., Ghio, S., Chen, J., Lai, C., Laguens, R. P., Lloyd, K. C., and Hertig, C.
575 M. (2005) Dilated cardiomyopathy in Erb-b4-deficient ventricular muscle. *Am. J.*
576 *Physiol. Heart Circ. Physiol.* **289**, H1153-60
577 26. Montaigne, D., Hurt, C., and Neviere, R. (2012) Mitochondria Death/Survival
578 Signaling Pathways in Cardiotoxicity Induced by Anthracyclines and Anticancer-
579 Targeted Therapies. *Biochem. Res. Int.* **2012**, 1–12
580 27. Lemmens, K., Segers, V. F. M., Demolder, M., and De Keulenaer, G. W. (2006) Role
581 of neuregulin-1/ErbB2 signaling in endothelium-cardiomyocyte cross-talk. *J. Biol.*
582 *Chem.* **281**, 19469–19477
583 28. Campreciós, G., Sánchez-Vizcaíno, E., Soley, M., and Ramírez, I. (2011) Chronic β-
584 adrenergic stimulation increases ErbB receptors and cell proliferation in mouse kidney.
585 *Growth Factors* **29**, 94–101
586 29. Garrido, V., Mendoza-Torres, E., Riquelme, J. A., Díaz, A., Pizarro, M., Bustamante,
587 M., Chavez, M. N., Ocaranza, M. P., Mellado, R., Corbalan, R., Allende, M. L., and
588 Lavandero, S. (2017) Novel Therapies Targeting Cardioprotection and Regeneration.
589 *Curr. Pharm. Des.* **23**, 2592–2615
590 30. Lenneman, C. G. (2014) Neuregulin-1 Signaling in the Pathogenesis of Chemotherapy-
591 Induced Heart Failure. *Curr. Heart Fail. Rep.* **11**, 134–138
592 31. Sawyer, D. B. and Caggiano, A. (2011) Neuregulin-1β for the treatment of systolic
593 heart failure. *J. Mol. Cell. Cardiol.* **51**, 501–505
594 32. Wadugu, B. and Kühn, B. (2012) The role of neuregulin/ErbB2/ErbB4 signaling in the
595 heart with special focus on effects on cardiomyocyte proliferation. *Am. J. Physiol.*
596 *Circ. Physiol.* **302**, H2139–H2147
597 33. Odiete, O., Hill, M. F., and Sawyer, D. B. (2012) Neuregulin in cardiovascular
598 development and disease. *Circ. Res.* **111**, 1376–1385
599 34. De Keulenaer, G. W., Doggen, K., and Lemmens, K. (2010) The Vulnerability of the
600 Heart As a Pluricellular Paracrine Organ. *Circ. Res.* **106**, 35–46
601 35. Lemmens, K., Doggen, K., and De Keulenaer, G. W. (2007) Role of neuregulin-1/ErbB

signaling in cardiovascular physiology and disease: implications for therapy of heart failure. *Circulation* **116**, 954–960

36. Gao, R., Zhang, J., Cheng, L., Wu, X., Dong, W., Yang, X., Li, T., Liu, X., Xu, Y., Li, X., and Zhou, M. (2010) A Phase II, Randomized, Double-Blind, Multicenter, Based on Standard Therapy, Placebo-Controlled Study of the Efficacy and Safety of Recombinant Human Neuregulin-1 in Patients With Chronic Heart Failure. *J. Am. Coll. Cardiol.* **55**, 1907–1914

37. Jabbour, A., Hayward, C. S., Keogh, A. M., Kotlyar, E., McCrohon, J. A., England, J. F., Amor, R., Liu, X., Li, X. Y., Zhou, M. D., Graham, R. M., and Macdonald, P. S. (2011) Parenteral administration of recombinant human neuregulin-1 to patients with stable chronic heart failure produces favourable acute and chronic haemodynamic responses. *Eur. J. Heart Fail.* **13**, 83–92

38. Lim, S. L., Lam, C. S. P., Segers, V. F. M., Brutsaert, D. L., and De Keulenaer, G. W. (2015) Cardiac endothelium–myocyte interaction: clinical opportunities for new heart failure therapies regardless of ejection fraction. *Eur. Heart J.* **36**, 2050–2060

39. Vandekerckhove, L., Vermeulen, Z., Liu, Z. Z., Boimvaser, S., Patzak, A., Segers, V. F. M., and De Keulenaer, G. W. (2016) Neuregulin-1 attenuates development of nephropathy in a type 1 diabetes mouse model with high cardiovascular risk. *Am. J. Physiol. Endocrinol. Metab.* **310**, E495-504

40. Coaxum, S. D., Garnovskaya, M. N., Gooz, M., Baldys, A., and Raymond, J. R. (2009) Epidermal growth factor activates Na(+/)H(+) exchanger in podocytes through a mechanism that involves Janus kinase and calmodulin. *Biochim. Biophys. Acta* **1793**, 1174–1181

41. Harris, R. C. (1989) Response of rat inner medullary collecting duct to epidermal growth factor. *Am. J. Physiol. Physiol.* **256**, F1117–F1124

42. Zhao, X., Lu, X., and Feng, Q. (2002) Deficiency in endothelial nitric oxide synthase impairs myocardial angiogenesis. *Am. J. Physiol. - Hear. Circ. Physiol.* **283**

43. Stauss, H. M., Nafz, B., Mrowka, R., and Persson, P. B. (2000) Blood pressure control in eNOS knock-out mice: Comparison with other species under NO blockade.

44. Li, W., Mital, S., Ojaimi, C., Csiszar, A., Kaley, G., and Hintze, T. H. (2004) Premature death and age-related cardiac dysfunction in male eNOS-knockout mice. *J. Mol. Cell. Cardiol.* **37**, 671–680

45. Whiting, C., Castillo, A., Haque, M. Z., and Majid, D. S. A. (2013) Protective role of

the endothelial isoform of nitric oxide synthase in ANG II-induced inflammatory responses in the kidney. *Am. J. Physiol. Renal Physiol.* **305**, F1031-41

46. Simmons, L. J., Surles-Zeigler, M. C., Li, Y., Ford, G. D., Newman, G. D., and Ford, B. D. (2016) Regulation of inflammatory responses by neuregulin-1 in brain ischemia and microglial cells in vitro involves the NF-kappa B pathway. *J. Neuroinflammation* **13**

47. Liu, X., Gu, X., Li, Z., Li, X., Li, H., Chang, J., Chen, P., Jin, J., Xi, B., Chen, D., Lai, D., Graham, R. M., and Zhou, M. (2006) Neuregulin-1/erbB-Activation Improves Cardiac Function and Survival in Models of Ischemic, Dilated, and Viral Cardiomyopathy. *J. Am. Coll. Cardiol.* **48**, 1438–1447

48. Lu, T. P., Lee, C. Y., Tsai, M. H., Chiu, Y. C., Hsiao, C. K., Lai, L. C., and Chuang, E. Y. (2012) MiRSystem: An integrated system for characterizing enriched functions and pathways of microRNA targets. *PLoS One* **7**

49. Ludwig, N., Leidinger, P., Becker, K., Backes, C., Fehlmann, T., Pallasch, C., Rheinheimer, S., Meder, B., Stähler, C., Meese, E., and Keller, A. (2016) Distribution of miRNA expression across human tissues. *Nucleic Acids Res.* **44**, 3865–3877

50. Sticht, C., De La Torre, C., Parveen, A., and Gretz, N. (2018) miRWalk: An online resource for prediction of microRNA binding sites. *PLoS One* **13**, e0206239

51. Hodgin, J. B., Bitzer, M., Wickman, L., Afshinnia, F., Wang, S. Q., O'Connor, C., Yang, Y., Meadowbrooke, C., Chowdhury, M., Kikuchi, M., Wiggins, J. E., and Wiggins, R. C. (2015) Glomerular Aging and Focal Global Glomerulosclerosis: A Podometric Perspective. *J. Am. Soc. Nephrol.* **26**, 3162–3178

52. Rose, B. A., Force, T., and Wang, Y. (2010) Mitogen-Activated Protein Kinase Signaling in the Heart: Angels Versus Demons in a Heart-Breaking Tale. *Physiol. Rev.* **90**, 1507–1546

53. De Keulenaer, G. W., Segers, V. F. M., Zannad, F., and Brutsaert, D. L. (2017) The future of pleiotropic therapy in heart failure. Lessons from the benefits of exercise training on endothelial function. *Eur. J. Heart Fail.* **19**, 603–614

54. De Keulenaer, G. W., Segers, V. F. M., Zannad, F., and Brutsaert, D. L. (2017) The future of pleiotropic therapy in heart failure. Lessons from the benefits of exercise training on endothelial function. *Eur. J. Heart Fail.* **19**, 603–614

55. Vermeulen, Z., Mateiu, L., Dugaucquier, L., De Keulenaer, G. W., and Segers, V. F. M. (2019) Cardiac endothelial cell transcriptome in neonatal, adult, and remodeling

hearts. *Physiol. Genomics* **51**, 186–196

56. Lundberg, J. O., Gladwin, M. T., and Weitzberg, E. (2015) Strategies to increase nitric oxide signalling in cardiovascular disease. *Nat. Rev. Drug Discov.* **14**, 623–641

57. Forstermann, U. and Sessa, W. C. (2012) Nitric oxide synthases: regulation and function. *Eur. Heart J.* **33**, 829–837

58. Li, H., Horke, S., and Förstermann, U. (2014) Vascular oxidative stress, nitric oxide and atherosclerosis. *Atherosclerosis* **237**, 208–219

59. Kuhlencordt, P. J., Gyurko, R., Han, F., Scherrer-Crosbie, M., Aretz, T. H., Hajjar, R., Picard, M. H., and Huang, P. L. (2001) Accelerated atherosclerosis, aortic aneurysm formation, and ischemic heart disease in apolipoprotein E/endothelial nitric oxide synthase double-knockout mice. *Circulation* **104**, 448–454

60. Rudic, R. D., Shesely, E. G., Maeda, N., Smithies, O., Segal, S. S., and Sessa, W. C. (1998) Direct evidence for the importance of endothelium-derived nitric oxide in vascular remodeling. *J. Clin. Invest.* **101**, 731–736

61. Cook, S., Hugli, O., Egli, M., Ménard, B., Thalmann, S., Sartori, C., Perrin, C., Nicod, P., Thorens, B., Vollenweider, P., Scherrer, U., and Burcelin, R. (2004) Partial gene deletion of endothelial nitric oxide synthase predisposes to exaggerated high-fat diet-induced insulin resistance and arterial hypertension. *Diabetes* **53**, 2067–2072

62. Shankar, R. R., Wu, Y., Shen, H. Q., Zhu, J. S., and Baron, A. D. (2000) Mice with gene disruption of both endothelial and neuronal nitric oxide synthase exhibit insulin resistance. *Diabetes* **49**, 684–687

63. De Vito, P. (2014) Atrial natriuretic peptide: An old hormone or a new cytokine? *Peptides* **58**, 108–116

64. Hedhli, N., Huang, Q., Kalinowski, A., Palmeri, M., Hu, X., Russell, R. R., and Russell, K. S. (2011) Endothelium-derived neuregulin protects the heart against ischemic injury. *Circulation* **123**, 2254–2262

65. Gallo, S., Vitacolonna, A., Bonzano, A., Comoglio, P., and Crepaldi, T. (2019) ERK: A Key Player in the Pathophysiology of Cardiac Hypertrophy. *Int. J. Mol. Sci.* **20**, 2164

66. Gui, C., Zeng, Z. Y., Chen, Q., Luo, Y. W., Li, L., and Chen, L. L. (2018) Neuregulin-1 Promotes Myocardial Angiogenesis in the Rat Model of Diabetic Cardiomyopathy. *Cell. Physiol. Biochem.* **46**, 2325–2334

67. Zoja, C., Cattaneo, S., Fiordaliso, F., Lionetti, V., Zambelli, V., Salio, M., Corna, D., Pagani, C., Rottoli, D., Bisighini, C., Remuzzi, G., and Benigni, A. (2011) Distinct

cardiac and renal effects of eta receptor antagonist and ace inhibitor in experimental type 2 diabetes. *Am. J. Physiol. - Ren. Physiol.* **301**

68. Del Ry, S., Cabiati, M., Martino, A., Cavallini, C., Caselli, C., Aquaro, G. D., Battolla, B., Prescimone, T., Giannessi, D., Mattii, L., and Lionetti, V. (2013) High concentration of C-type natriuretic peptide promotes VEGF-dependent vasculogenesis in the remodeled region of infarcted swine heart with preserved left ventricular ejection fraction. *Int. J. Cardiol.* **168**, 2426–2434

69. Geisberg, C. A., Wang, G., Safa, R. N., Smith, H. M., Anderson, B., Peng, X.-Y., Veerkamp, B., Zhao, D. X., Blakemore, D., Yu, C., and Sawyer, D. B. (2011) Circulating neuregulin-1β levels vary according to the angiographic severity of coronary artery disease and ischemia. *Coron. Artery Dis.* **22**, 577–582

70. Geisberg, C. A., Abdallah, W. M., da Silva, M., Silverstein, C., Smith, H. M., Abramson, V., Mayer, I., Means-Powell, J., Freehardt, D., White, B., Lenihan, D., and Sawyer, D. B. (2013) Circulating neuregulin during the transition from stage A to stage B/C heart failure in a breast cancer cohort. *J. Card. Fail.* **19**, 10–15

71. Ky, B., Kimmel, S. E., Safa, R. N., Putt, M. E., Sweitzer, N. K., Fang, J. C., Sawyer, D. B., and Cappola, T. P. (2009) Neuregulin-1 beta is associated with disease severity and adverse outcomes in chronic heart failure. *Circulation* **120**, 310–317

72. Zurek, M., Johansson, E., Palmer, M., Albery, T., Johansson, K., Rydén-Markinhutha, K., and Wang, Q.-D. (2020) Neuregulin-1 Induces Cardiac Hypertrophy and Impairs Cardiac Performance in Post–Myocardial Infarction Rats. *Circulation* **142**, 1308–1311

73. Wang, X., Zhuo, X., Gao, J., Liu, H., Lin, F., and Ma, A. (2019) Neuregulin-1β partially improves cardiac function in volume-overload heart failure through regulation of abnormal calcium handling. *Front. Pharmacol.* **10**

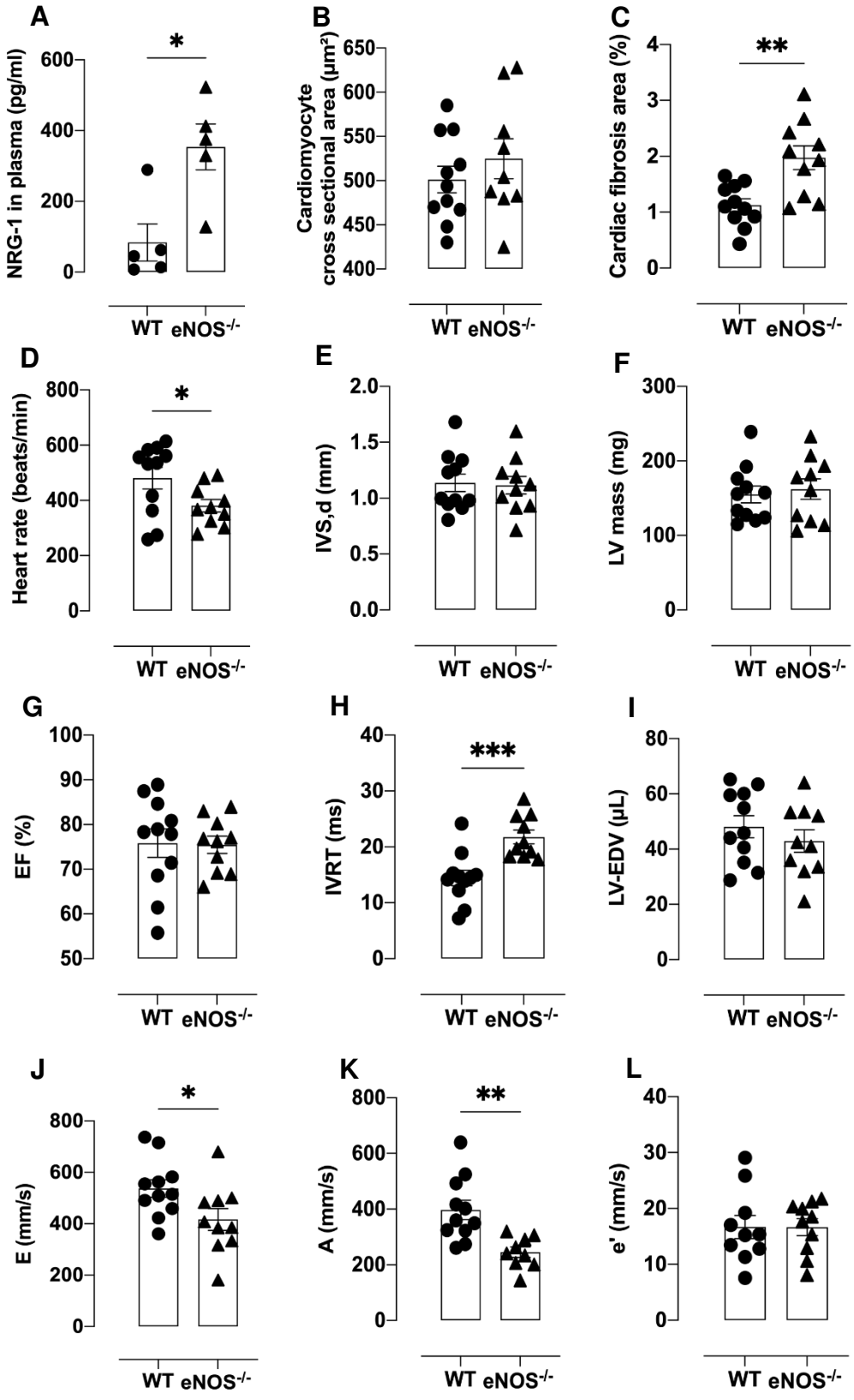
A
NRG-1 in plasma (pg/ml)
600
400
200
0
*
WT
eNOS-/-
B
Cardiomyocyte cross sectional area (µm²)
650
600
550
500
450
400
WT
eNOS-/-
C
Cardiac fibrosis area (%)
4
3
2
1
0
**
WT
eNOS-/-
D
Heart rate (beats/min)
800
600
400
200
0
*
WT
eNOS-/-
E
IVS,d (mm)
2.0
1.5
1.0
0.5
0.0
WT
eNOS-/-
F
LV mass (mg)
300
200
100
0
WT
eNOS-/-
G
EF (%)
100
90
80
70
60
50
WT
eNOS-/-
H
IVRT (ms)
40
30
20
10
0
***
WT
eNOS-/-
I
LV-EDV (µL)
80
60
40
20
0
WT
eNOS-/-
J
E (mm/s)
800
600
400
200
0
*
WT
eNOS-/-
K
A (mm/s)
800
600
400
200
0
**
WT
eNOS-/-
L
e' (mm/s)
40
30
20
10
0
WT
eNOS-/-

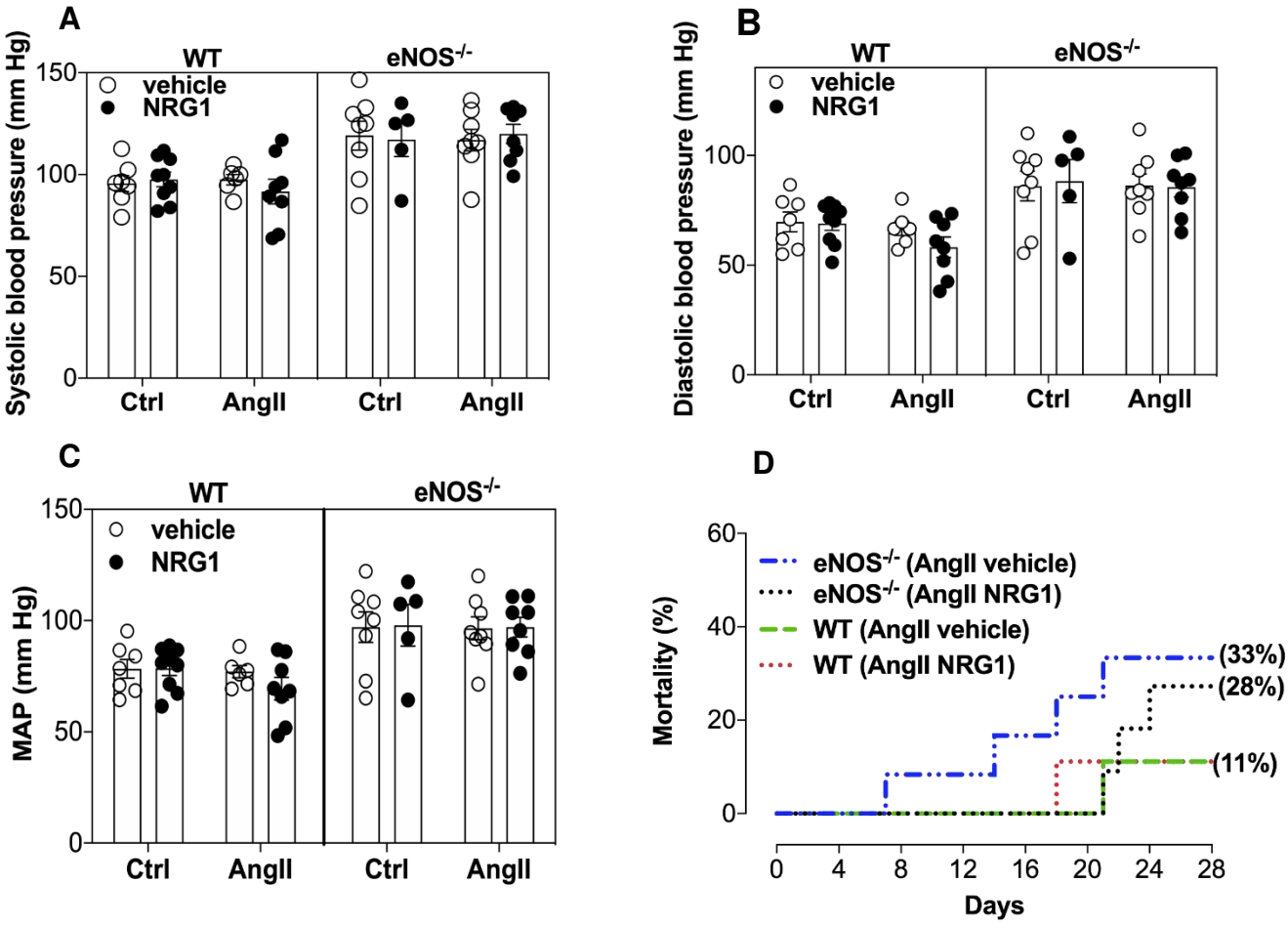
A
WT
eNOS-/-
vehicle
NRG1
Systolic blood pressure (mm Hg)
150
100
50
0
Ctrl
AngII
Ctrl
AngII
B
WT
eNOS-/-
vehicle
NRG1
Diastolic blood pressure (mm Hg)
100
50
0
Ctrl
AngII
Ctrl
AngII
C
WT
eNOS-/-
vehicle
NRG1
MAP (mm Hg)
150
100
50
0
Ctrl
AngII
Ctrl
AngII
D
eNOS-/- (AngII vehicle)
eNOS-/- (AngII NRG1)
WT (AngII vehicle)
WT (AngII NRG1)
(33%)
(28%)
(11%)
Mortality (%)
60
40
20
0
0
4
8
12
16
20
24
28
Days

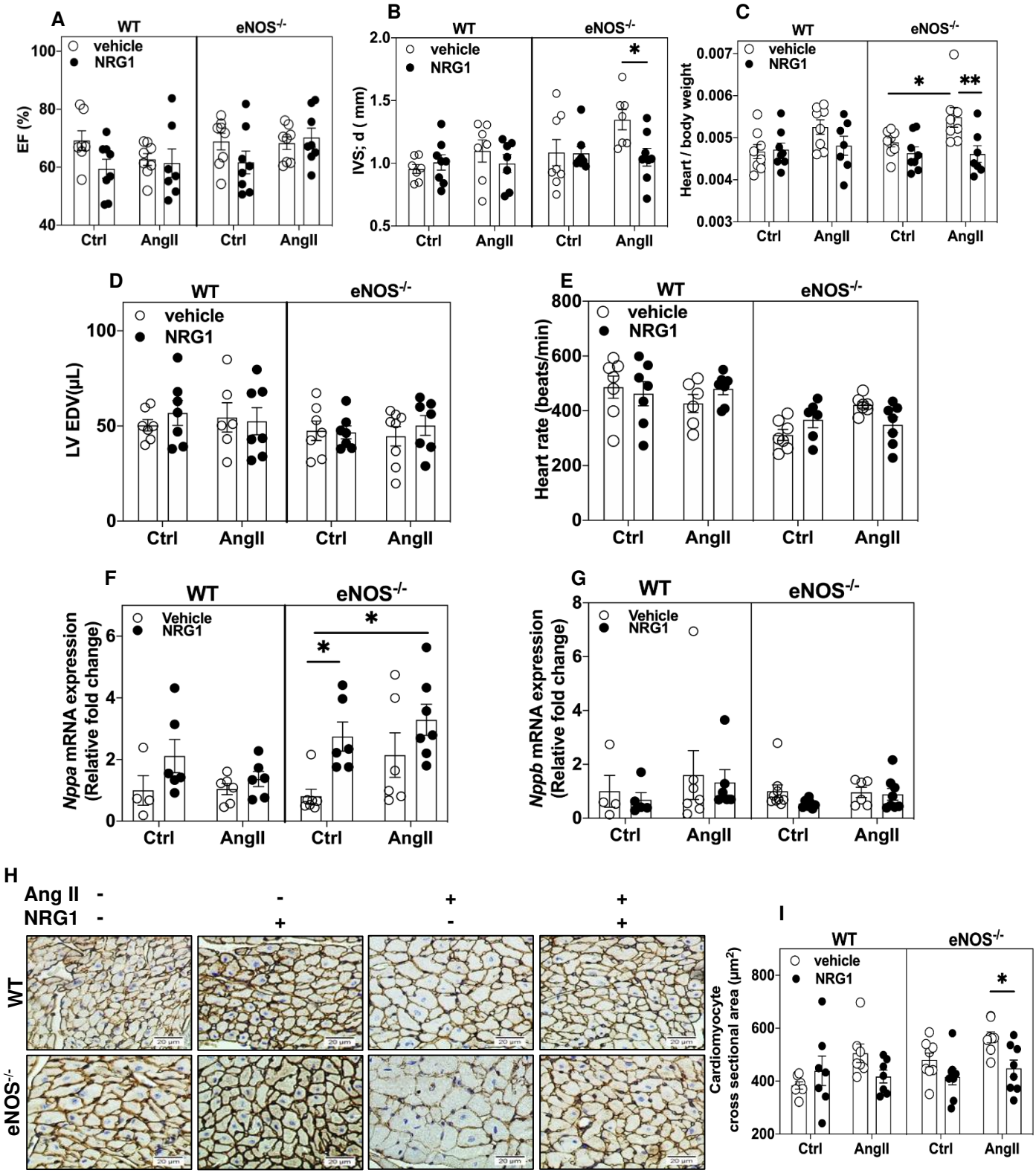
A
WT
eNOS-/-
vehicle
NRG1
EF (%)
100
80
60
40
Ctrl
AngII
B
IVS; d (mm)
2.0
1.5
1.0
0.5
*
C
Heart / body weight
0.007
0.006
0.005
0.004
0.003
*
**
D
LV EDV(μL)
100
50
0
E
Heart rate (beats/min)
800
600
400
200
0
F
Nppa mRNA expression
(Relative fold change)
Vehicle
NRG1
6
4
2
0
*
*
G
Nppb mRNA expression
(Relative fold change)
8
6
4
2
0
H
Ang II - - + +
NRG1 - + - +
WT
eNOS-/-
20 μm
I
Cardiomyocyte
cross sectional area (μm2)
800
600
400
200
*

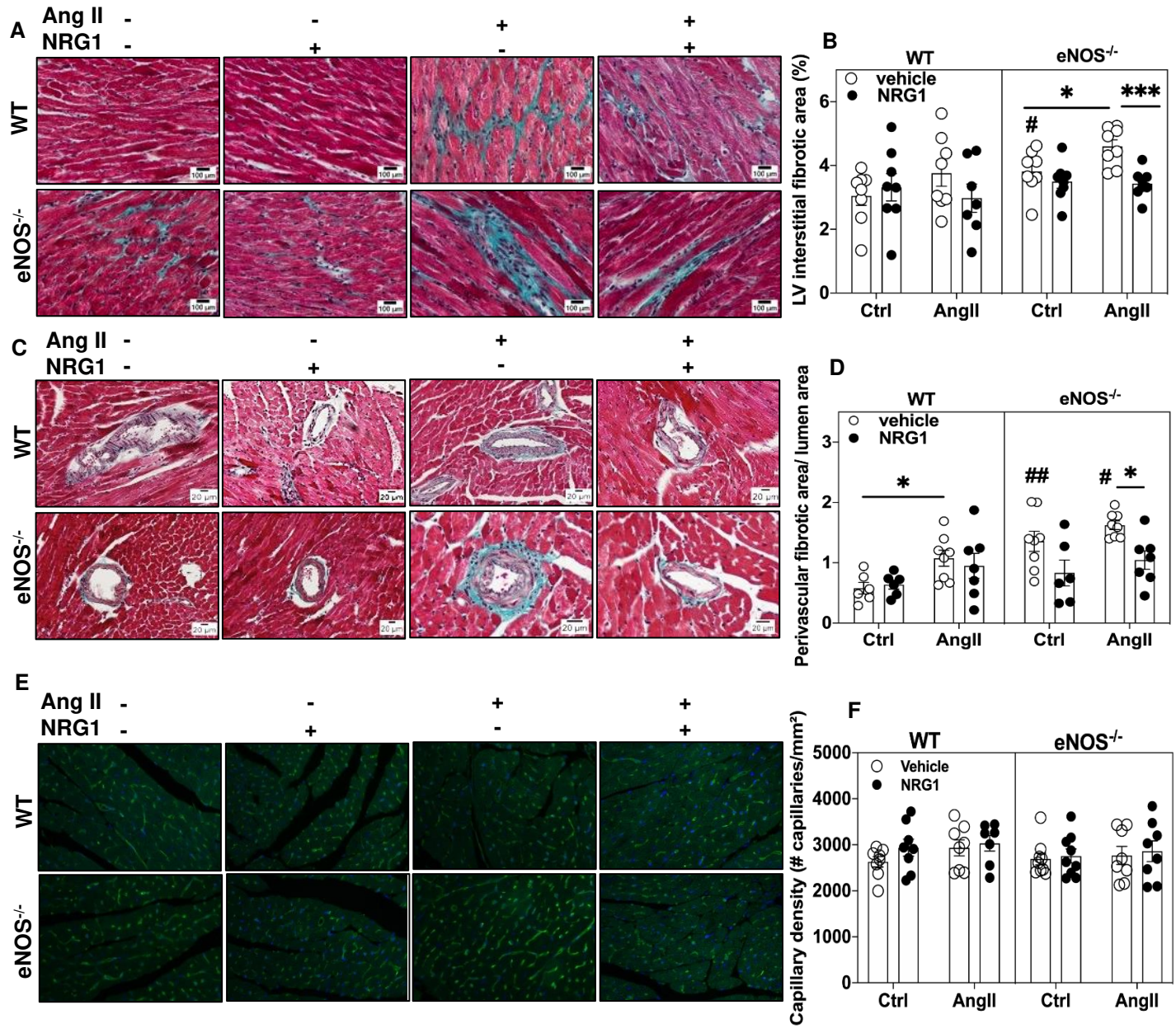
A
Ang II - - + +
NRG1 - + - +
WT
eNOS-/-
B
WT
eNOS-/-
vehicle
NRG1
LV interstitial fibrotic area (%)
Ctrl
AngII
C
D
Perivascular fibrotic area/ lumen area
E
F
Vehicle
Capillary density (# capillaries/mm²)

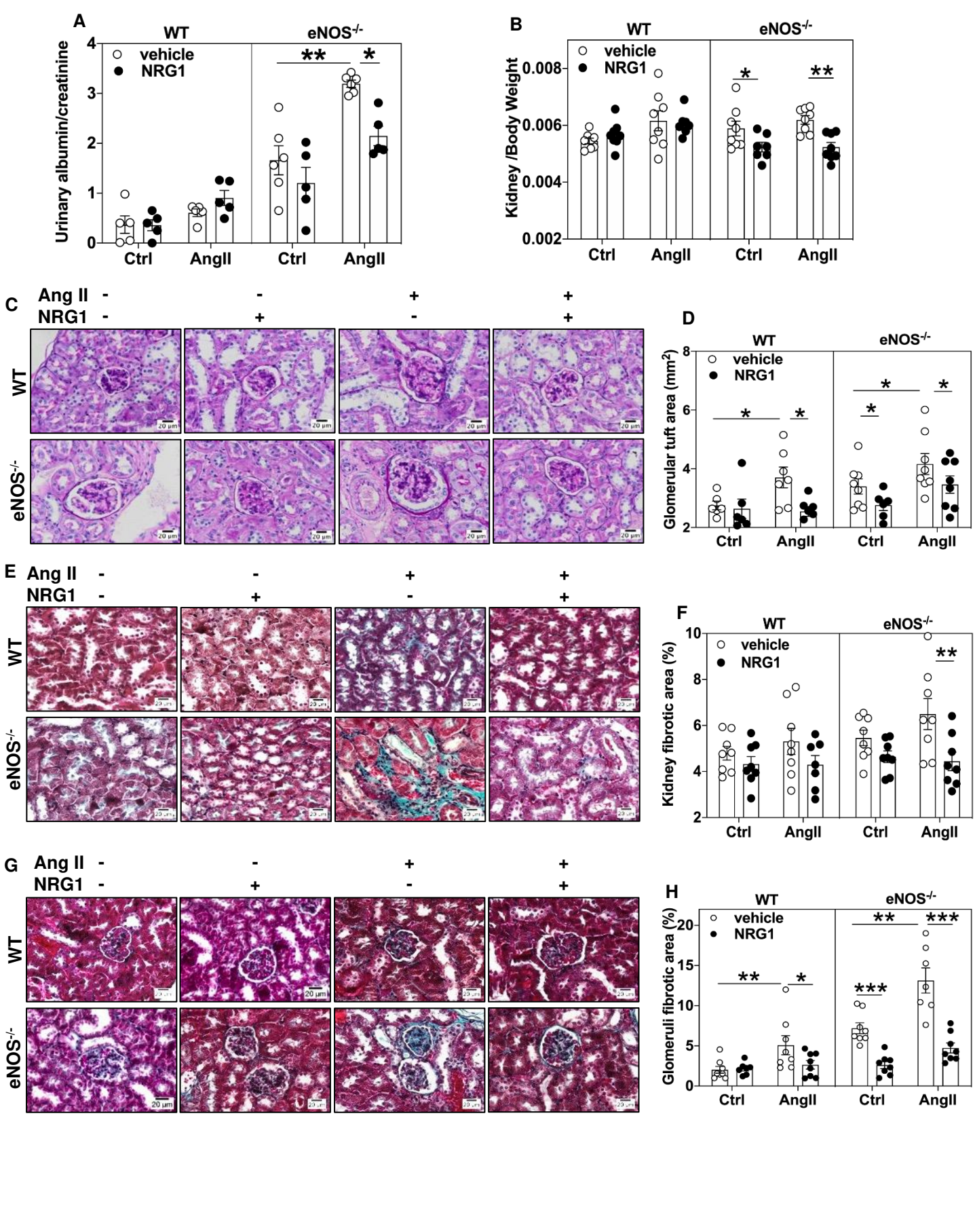
A
WT
eNOS-/-
vehicle
NRG1
Urinary albumin/creatinine
Ctrl
AngII
B
Kidney /Body Weight
C
Ang II
NRG1
WT
eNOS-/-
D
Glomerular tuft area (mm2)
E
F
Kidney fibrotic area (%)
G
H
Glomeruli fibrotic area (%)

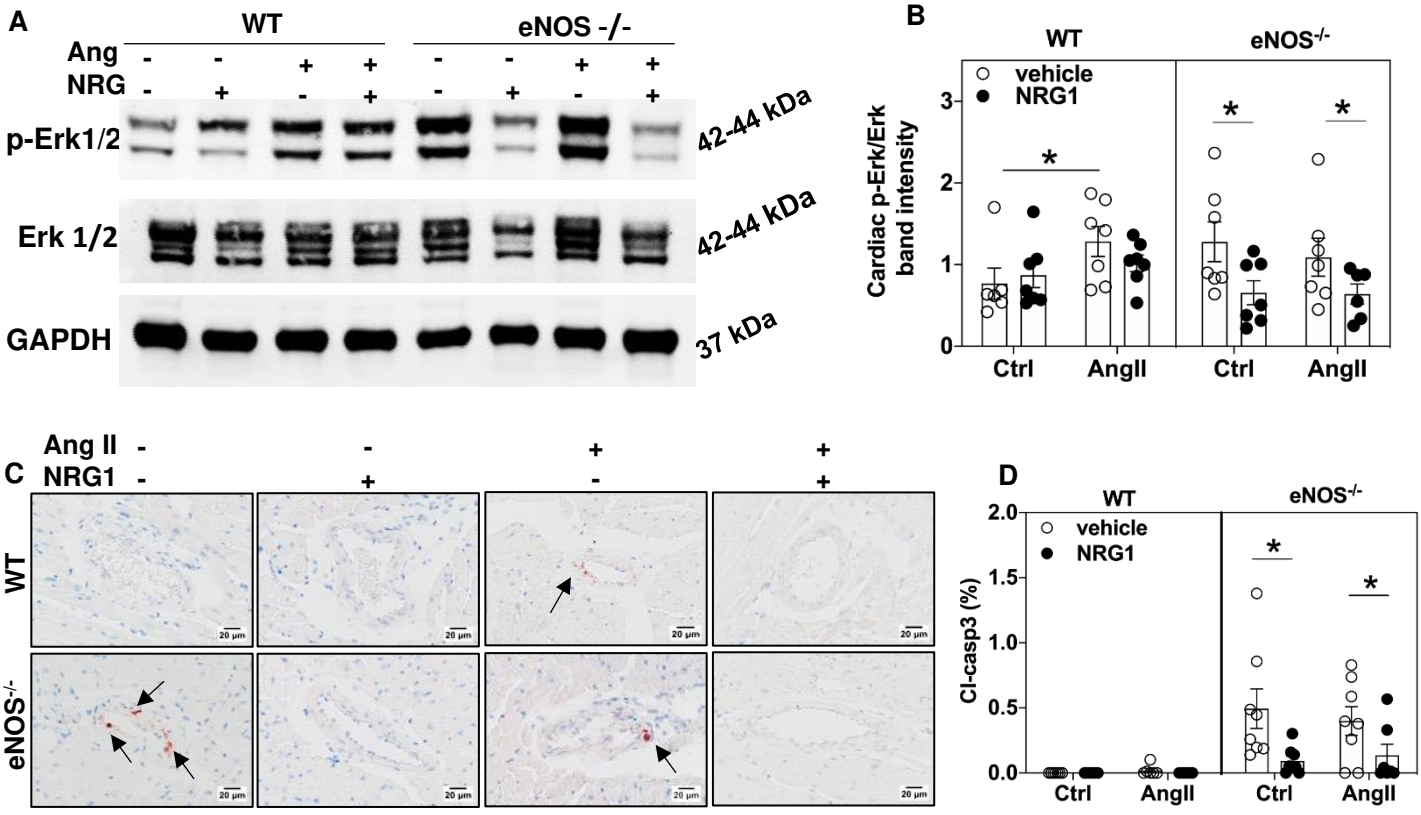
A
WT
eNOS -/-
Ang
NRG
p-Erk1/2
Erk 1/2
GAPDH
42-44 kDa
42-44 kDa
37 kDa
B
WT
eNOS-/-
vehicle
NRG1
Cardiac p-Erk/Erk band intensity
Ctrl
AngII
Ctrl
AngII
C
Ang II
NRG1
WT
eNOS-/-
20 µm
D
WT
eNOS-/-
vehicle
NRG1
Cl-casp3 (%)
Ctrl
AngII
Ctrl
AngII

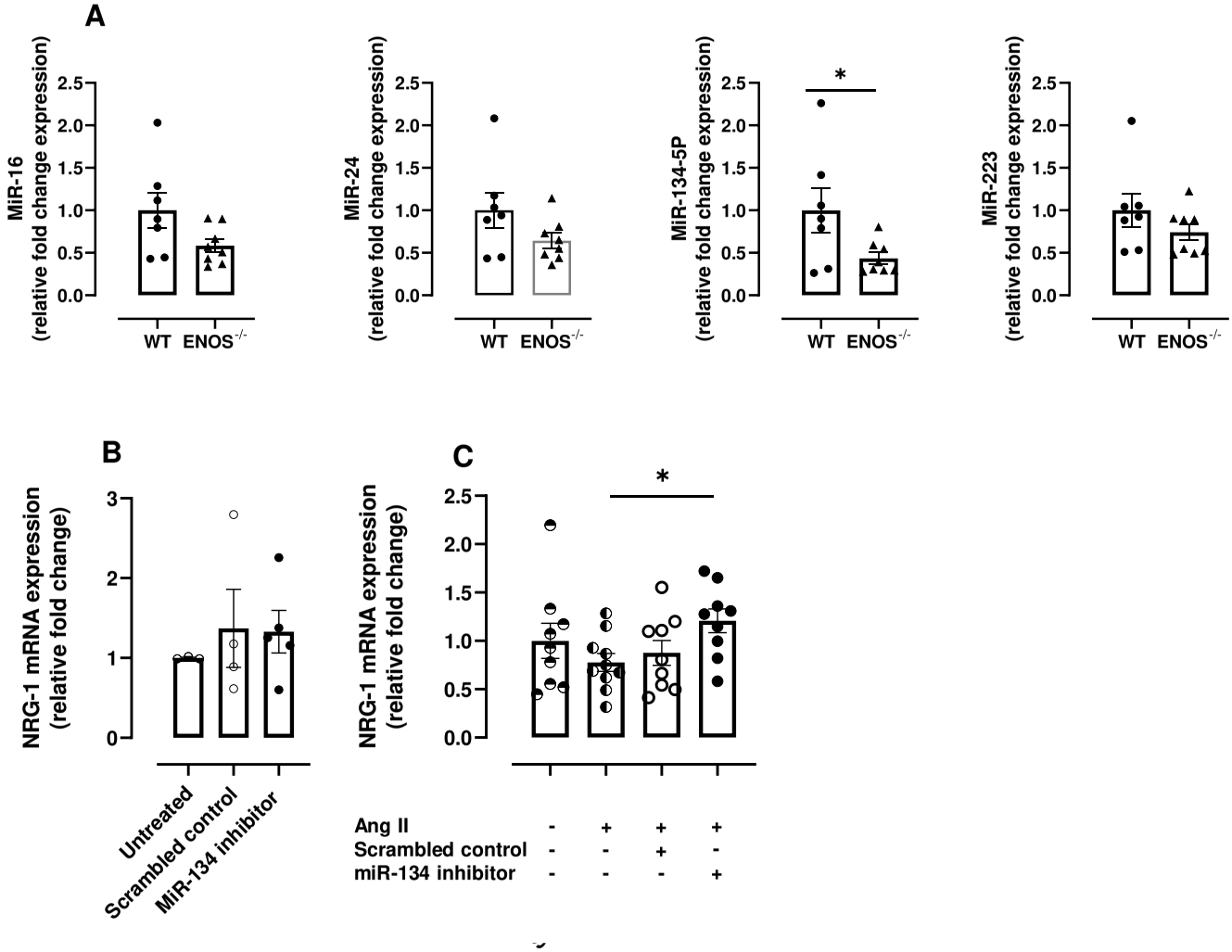
A
MiR-16
(relative fold change expression)
2.5
2.0
1.5
1.0
0.5
0.0
WT
ENOS-/-
MiR-24
(relative fold change expression)
MiR-134-5P
(relative fold change expression)
*
MiR-223
(relative fold change expression)
B
NRG-1 mRNA expression
(relative fold change)
3
2
1
0
Untreated
Scrambled control
MiR-134 inhibitor
C
NRG-1 mRNA expression
(relative fold change)
*
Ang II - + + +
Scrambled control - - + -
miR-134 inhibitor - - - +